

To aspirate or not to aspirate – impact of active versus passive ventilation on urban heat (island) indicators

Koen De Ridder, Bino Maiheu*, Dirk Lauwaet

VITO – Flemish Institute for Technological Research, Mol, Belgium

*Now at VMM – Flemish Environment Agency

Correspondence to: koen.deridder@vito.be

Keywords: measured temperature, mechanical aspiration, urban heat indicators

Abstract

The present paper reports on the impact of ventilation mode – active versus passive – of instrument screens for air temperature measurements on canopy urban heat (island) indicators. This is done using air temperature data gathered in the Antwerp (Belgium) area in July 2013, in an experimental set-up composed of an urban and a nearby rural climate station, each equipped with both actively and passively ventilated temperature sensors. The resulting data shows an air temperature bias between the passively and actively ventilated measurements of up to approximately 2°C, the highest values occurring under conditions of a high solar radiation load and low wind speed. Yet, the canopy urban heat island (UHI) increment, i.e., the urban-rural air temperature difference, is hardly affected by the ventilation method, which is ascribed to the fact that high UHI increments occur mainly at night when, in absence of solar radiation, active ventilation has a lesser influence on measured temperature. Conversely, urban heat indicators involving daytime air temperature, such as heatwave degree days (HWDD) or Steadman's apparent temperature, tend to produce overly high values when use is made of passively ventilated temperature measurements.

Keywords: temperature measurement, mechanical ventilation, urban heat indicator

1 Introduction

The combined effects of global climate change, the urban heat island (UHI) phenomenon, and urban population growth are expected to lead to an increased occurrence of excessive urban heat, causing adverse impacts on human health, labour productivity, infrastructure, and energy consumption, among other. In the pursuit of enhancing the scientific understanding of urban climate in general and the UHI effect in particular, near-surface (2-m) air temperature observations play an important role, either providing insights directly or else through the generation of reference data for numerical model validation.

Air temperature measurements are gathered routinely using temperature sensors encased in a radiation shield, which protects the sensor from direct exposure to solar radiation to reduce the radiation-induced bias to a minimum. Still, radiation shields cannot avoid this bias altogether, despite designs that allow air to enter and provide (natural) ventilation to the encased sensor. Indeed, the residual radiation effect may heat up the air in the protective shield by up to several °C, depending on the level of natural ventilation and the solar and thermal infrared radiation load (see, e.g., Nakamura and Mahrt, 2005; Erell et al., 2005).

Actively ventilated (aspirated) radiation shields are much less prone to such radiative heating, thanks to the use of mechanical ventilation, which forces air through the interior of the shield, bringing a constant flow of ambient air to the sensor, thus minimizing radiation effects (WMO, 2018). Hence, in principle, actively ventilated radiation shields are the preferred means to ensure minimally biased air temperature measurements. Yet, actively ventilated shields are more expensive, and require electrical power to run the ventilator. This causes logistical challenges such as the requirement to have access to an on-site electrical outlet, or the provision of a large battery coupled to a photovoltaic panel.

Hence, while naturally ventilated air temperature measurements are easier to implement than mechanically aspirated ones, this comes at the price of a lesser accuracy. Even though correction methods do exist (Nakamura and Mahrt, 2005; Mauder et al., 2008; Cheng et al., 2014), these are hampered by the requirement of having to continuously monitor other variables than temperature, such as short- and longwave radiation intensity and wind speed. Also, such corrections are not universal; instead, they depend on the shape and dimensions of the radiation shield and the temperature sensor and on the experimental site (e.g., degree of natural sheltering), requiring a careful calibration for every individual set-up.

Several investigations provide estimates of the radiation-induced temperature bias measured in naturally ventilated radiation shields, in as different environments as the Antarctic plateau (Morino et al., 2021), tropical mountain glaciers (Georges and Kaser, 2002), ocean buoys (Anderson and Baumgartner, 1998), and inside greenhouses (Ramesh and Arakeri, 2019).

Only a few studies have considered the urban environment. Among those, Erell et al. (2005) experimentally assessed the effect of active versus passive ventilation on measured temperature in an urban setting, finding differences amounting to 2.5°C. Gubler et al. (2021) investigated passively ventilated low-cost sensors in Bern, Switzerland, finding biases of up to approximately 2°C compared to temperature observations from reference stations using active ventilation. Finally, Terando et al. (2017) found that, when the urban impervious surface cover increases, non-aspirated shields considerably amplify the bias of recorded temperatures.

While these urban studies addressed the impact of active versus passive ventilation on measured air temperature in urban settings, to our best knowledge, no assessment has been made of the impact on canopy urban heat (island) indicators, whence the scope of the present study.

The remainder of this paper is organized as follows. Section 2 describes the experimental sites and the instruments used to compare actively and passively ventilated air temperature measurements. Section 3 presents observed temperature values at these locations, highlighting the differences between the actively and passively ventilated measurements, focusing on indicators of the urban thermal environment and on urban-rural temperature differences, and discussing causes for the observed temperature biases. Section 4 presents the conclusions.

2 Materials and methods

In this study, use was made of measurements collected through two Campbell Scientific climate stations located in northern Belgium, one in the city of Antwerp and another in a nearby rural location (see Figure 1 and Table 1; also see the Appendix).

The wider agglomeration of Antwerp counts approximately one million inhabitants, and is built around a core of compact mid-rise buildings, surrounded by compact low-rise and, towards its periphery, open low-rise built areas. (Figure A1 of the Appendix shows the spatial distribution of the Local Climate Zones occurring within the study domain.) In the north, a large harbour area, the port of Antwerp, is

situated. In most other directions, the city is surrounded by moderately densely built areas, intermixed with pastures, cropland, and small forest patches. The study domain is flat, with height variations of less than 20 metres. The region enjoys a temperate maritime climate (Köppen type Cfb), with mild winters, mild summers, and precipitation all year round.

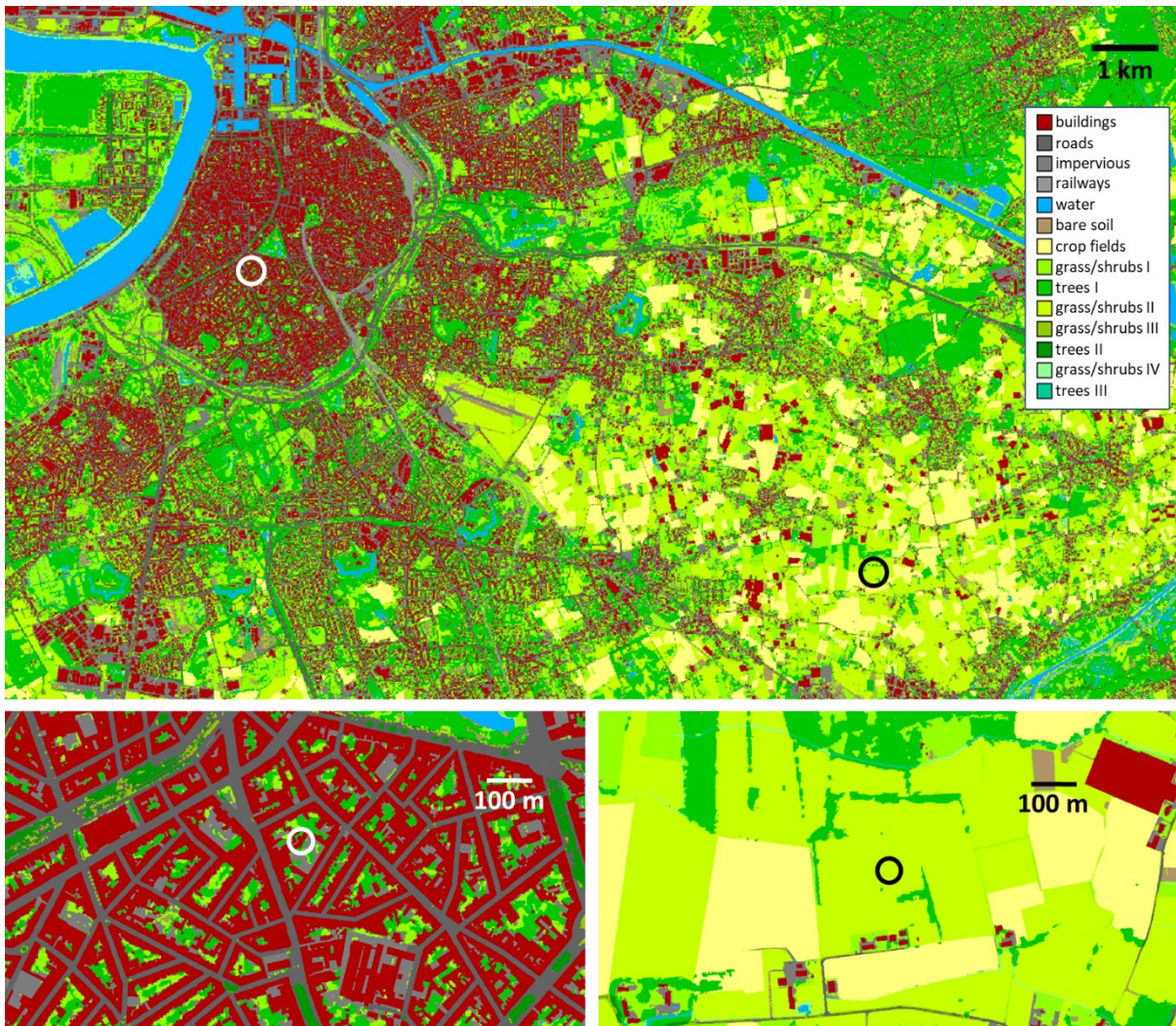


Figure 1. Upper panel: land cover map of the study domain, with the city of Antwerp in the upper left quadrant. The position of the urban and rural stations is marked with a white and a black circle, respectively. Lower panels: details of the land cover surrounding the urban (left) and rural (right) climate stations. Source: Geopunt Vlaanderen, 1-m land cover map for 2012, <https://www.geopunt.be/>.

The two climate stations were set up in July 2012, with the intention mainly to generate measurement data for model validation (De Ridder et al., 2015) and for establishing urban-rural heat indicators for the Flemish Environment Agency (Brouwers et al., 2015). The sites, which are 10.8 km apart, were carefully selected to be as representative as possible of their surroundings (also see Table 1 and information presented in the Appendix):

- The **urban station** is located on top of a small 4.5-m high building bordering a school's playground, and is generally embedded in an area with compact mid-rise buildings. Since the temperature measurements are conducted at a height of 1.8 m above the climate station's basis, the effective measurement height is 6.3 m above ground level. Most of the surrounding buildings extend to approximately 17 m height (range 13.5-26 m), hence this 6.3-m measurement height can be considered representative of urban canopy conditions. (Note that

all building and ground-level heights level were determined from the Digital Surface Model (DHMVII_DSM_1m) provided by Geopunt Vlaanderen, <https://www.geopunt.be/>). The station sits on top of a roof approximately 30 m long by 10 m wide, the station (Figure A2) being positioned at 2.5 m from the roof's edge and 10 m from the nearest wall.

- The **rural station** is located in the middle of a pasture area, with a few scattered trees at 60 m distance and some low buildings at 150 m, and otherwise mainly surrounded by rural agricultural and (semi-)natural land for kilometres in most directions, mostly low vegetation interspersed with scattered forest patches. Here also, the temperature sensors measure at a height of approximately 1.8 m above the ground.

More information regarding the stations' surroundings in terms of the Local Climate Zones (LCZ) classification (Stewart and Oke, 2012) and in terms of the immediate surroundings is provided in the Appendix. Also, below we provide more information regarding the representativeness of the urban station for the wider urban canopy beyond its precise location.

Table 1. Site information of the urban and rural climate stations (latitude, longitude, height above mean sea level), together with the land cover characteristics of the respective surrounding areas, based on the Local Climate Zones (LCZ) classification (Stewart and Oke, 2012; see the Appendix).

station	lat (°N) - lon (°E)	h (m above mean sea level)	land cover type
urban	51.20852° - 4.41026°	7.5 m	compact mid-rise urban (LCZ 2); average building height 17 m; scattered trees
rural	51.16600° - 4.54871°	11.4 m	low vegetation (LCZ D) (pasture); some scattered trees at 60 m; nearest building at approximately 150 m

The focus period of the study is the month of July 2013, which is the only full summer for which measurements were obtained at this urban site. The selected period is characterized by several hot days with temperatures well in excess of 30°C. This period also presents a fair variation in solar radiation intensity and wind speed, both of which are presumed drivers of the difference between actively and passively ventilated temperature measurements.

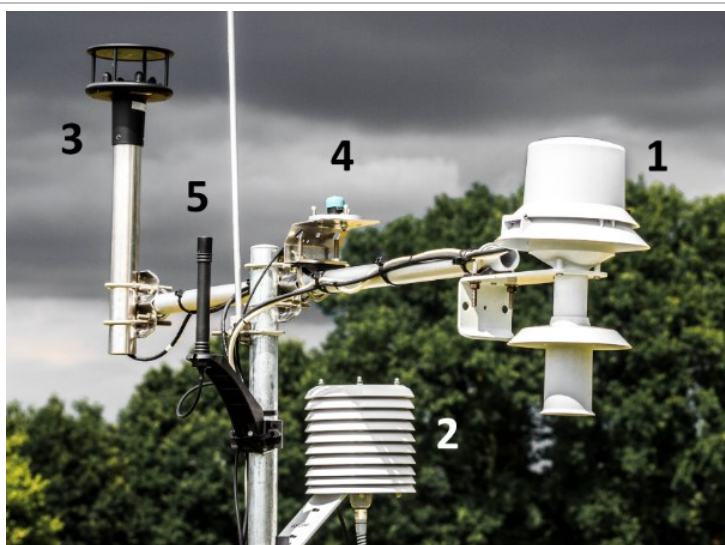


Figure 2. Instruments included in the urban and rural climate stations: (1) actively ventilated temperature sensor, (2) passively ventilated temperature-humidity sensor, (3) 2-D sonic anemometer, (4) shortwave radiation intensity sensor. The device labelled (5) is the GPRS antenna for the wireless data transmission. Note that the inlet of the actively ventilated radiation shield (1) is at the same height (1.8 m) as the centre of the louvred section of the passively ventilated shield (2). The 2-D sonic anemometer is positioned at approximately 2.4 m height.

The measurements were conducted by means of two identical professional-grade (Campbell Scientific) climate stations, one of each installed at the urban and rural locations described previously, and equipped with sensors measuring temperature, humidity, wind speed, and solar radiation intensity (Figure 2). In each of the two stations, temperature was measured both within passively and actively ventilated radiation shields. The air inlet of the latter was at the same height (1.8 m above the ground) as the average height of the louvred section of the passively ventilated device.

Table 2. Characteristics of the sensors used in the present study. Accuracy values were taken from the specifications provided by the manufacturer. The numbering in the leftmost column corresponds to that used in Figure 2.

Quantity	Sensor	Accuracy	Remarks
1 aspirated temperature	Campbell RTD43347	$\pm 0.2^{\circ}\text{C}$	Young 43502 aspirated shield
2 unaspirated temperature & relative humidity	Campbell CS215	$\pm 0.4^{\circ}\text{C}$ (T) $\pm 2\%$ (RH)	MET20 unaspirated shield
4 wind speed	Gill WindSonic	$\pm 2\%$	Ultrasonic wind probe
5 solar radiation intensity	Campbell CS300	$\pm 5\%$	Wavelengths 360-1120 nm

Measurements of all meteorological quantities occurred at 5-second intervals, and the resulting data were aggregated to 15-minute averages, which were logged onto Campbell Scientific CR800 data loggers and subsequently transferred to a central data server through a GPRS protocol. In addition to the climate data, the stations also logged the fan speed of the radiation shield's ventilator, which was monitored with respect to the proper functioning of the mechanical aspiration.

Prior to their deployment in the experimental sites, both climate stations were co-located during a few weeks on a small grass field, to verify differences in the measurements stemming from the pairwise identical temperature probes. It was found that the root mean squared difference between the temperature measurements amounted to 0.03°C for the actively ventilated probes and 0.3°C for the passively ventilated probes, i.e., well below the accuracy estimates provided by the manufacturer (Table 2).

To end this section, it should be noted that, while the rural site exhibits a large fetch in all directions and is located within an environment that is fairly representative of the wider surrounding area, the urban station's location may cause concerns with respect to its spatial representativeness. To understand this better, we compared the measurements conducted at the urban (school) location with concurrent measurements obtained at an urban (street) site 1.5 km away (51.20942°N , 4.43167°E), located within an overall similar environment (LCZ 'compact mid-rise'), yet with a rather different direct surrounding, one side of the station yielding to a broad open boulevard. At this secondary site, measurements were conducted at 4.5 m above ground level, using a HOBO U23-002 Pro v2 logger operating within the same type of actively ventilated radiation shield as at the main urban (school) site. The HOBO temperature logger had previously been compared to the Campbell RTD 43347 measurements, exhibiting a root mean square difference of 0.06°C , meaning that – for all practical purposes – both temperature measurement methods can be considered identical.

Lauwaet et al. (2013) show that temperature collected at both urban stations reveals near-coinciding temperatures at all times (see their Fig. 6). Also, Table 2 of Lauwaet et al. (2013) shows only minor differences in terms of the observed UHI intensity values, the average daytime values reaching 0.87°C

resp. 0.74°C , while during the night the values are 2.84°C resp. 2.94°C ; hence, we find very small differences between the two urban stations indeed. In conclusion, the fact that both urban stations yield very similar results inspires confidence in either station's representativeness of the LCZ category 'compact mid-rise' in Antwerp.

3 Results and discussion

Figure 3 and Figure 4 show time series of the measured meteorological quantities for the week of 18-24 July 2013, at 15-minute intervals, for the urban and rural sites, respectively.

In the urban measurements (Figure 3), temperatures are found to reach approximately 35°C during the period 21-23 July, night-time temperatures reaching around 20°C . The passively and actively ventilated temperatures differ by as much as 2°C , exhibiting a clear diurnal cycle with a daytime maximum. Wind speed values mostly remain in the range of $0.1\text{-}2\text{ ms}^{-1}$, also showing a distinct diurnal variation. The rural measurements (Figure 4) shown an altogether very similar picture, albeit with markedly higher wind speeds, exceeding 4 ms^{-1} at times, and exhibiting more variety throughout the study period than urban wind. Again, passively ventilated air temperature measurements exceed actively ventilated measurements by up to about 2°C , although to a lesser degree than is the case in the urban station. Note that the biases observed in both stations are consistent with values found by Erell et al. (2005), who obtained biases up to 2.5°C , their slightly higher value probably being related to a more intense shortwave radiation flux (around 1000 Wm^{-2} in their study compared to 800 Wm^{-2} in ours).

Occasionally, at night, the temperature difference becomes negative, i.e., the passively ventilated measurement yields the lower values, by up to around 1°C . These episodes appear to coincide with times of very low nocturnal wind speeds, which would suggest a radiative cause, the shield's casing becoming colder than the ambient air because of longwave radiative cooling. However, this night-time anomalous effect is stronger in the urban than in the rural measurements, which goes against what would be expected, considering that nocturnal longwave cooling should be more prominent in the rural site, which has a much larger sky-view factor than the urban site. Given the absence of longwave or net-radiation measurements, we refrain from any further speculations regarding the cause of this nocturnal phenomenon.

urban station

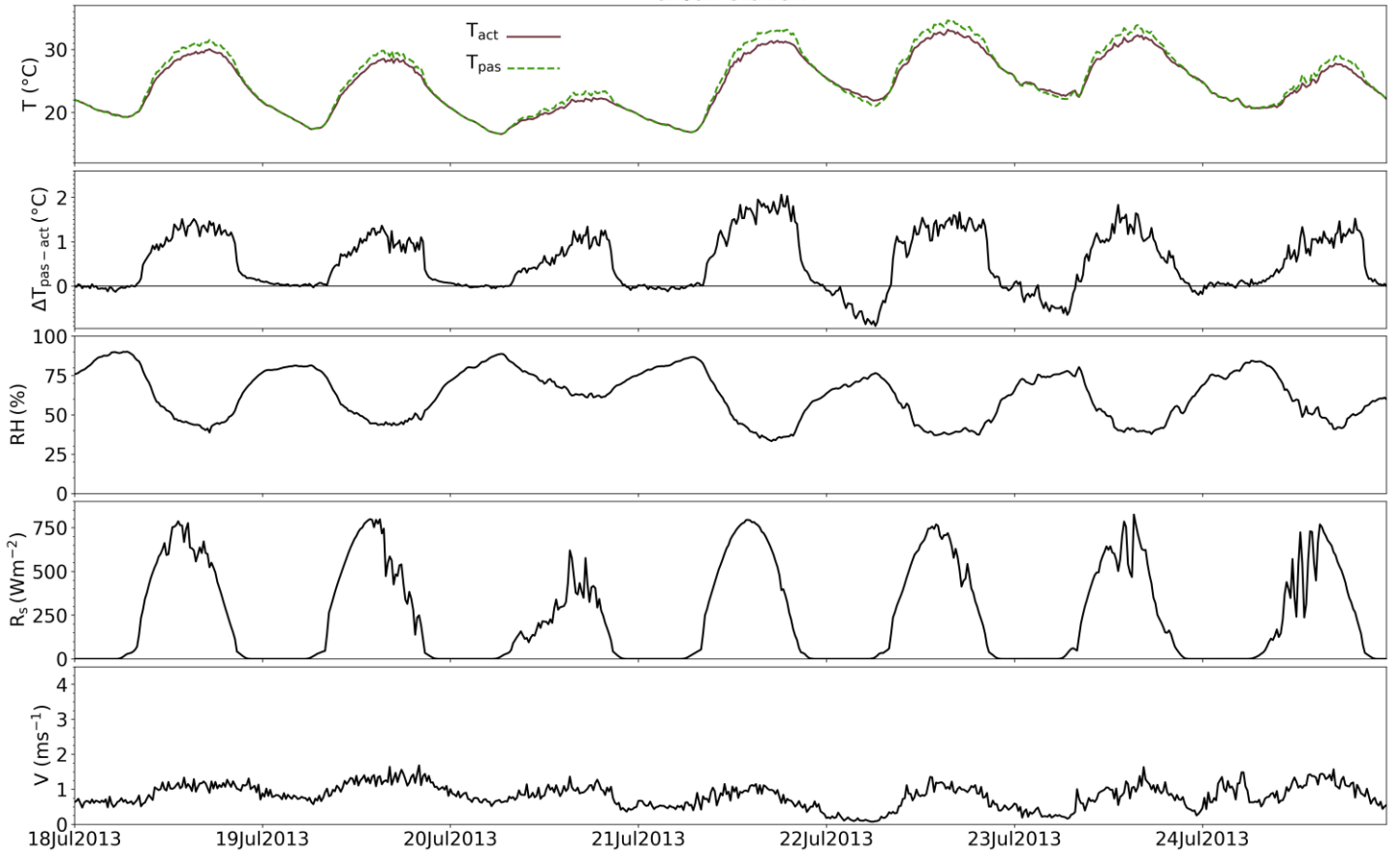


Figure 3. Climate variables measured at the urban station in the week of 18-24 July 2013 with, from top to bottom, actively (purple line) and passively (dashed green line) ventilated temperature (T); passively minus actively ventilated temperature difference ($\Delta T_{pas-act}$); relative humidity (RH); surface downwelling shortwave radiation (R_s); wind speed (V).

rural station

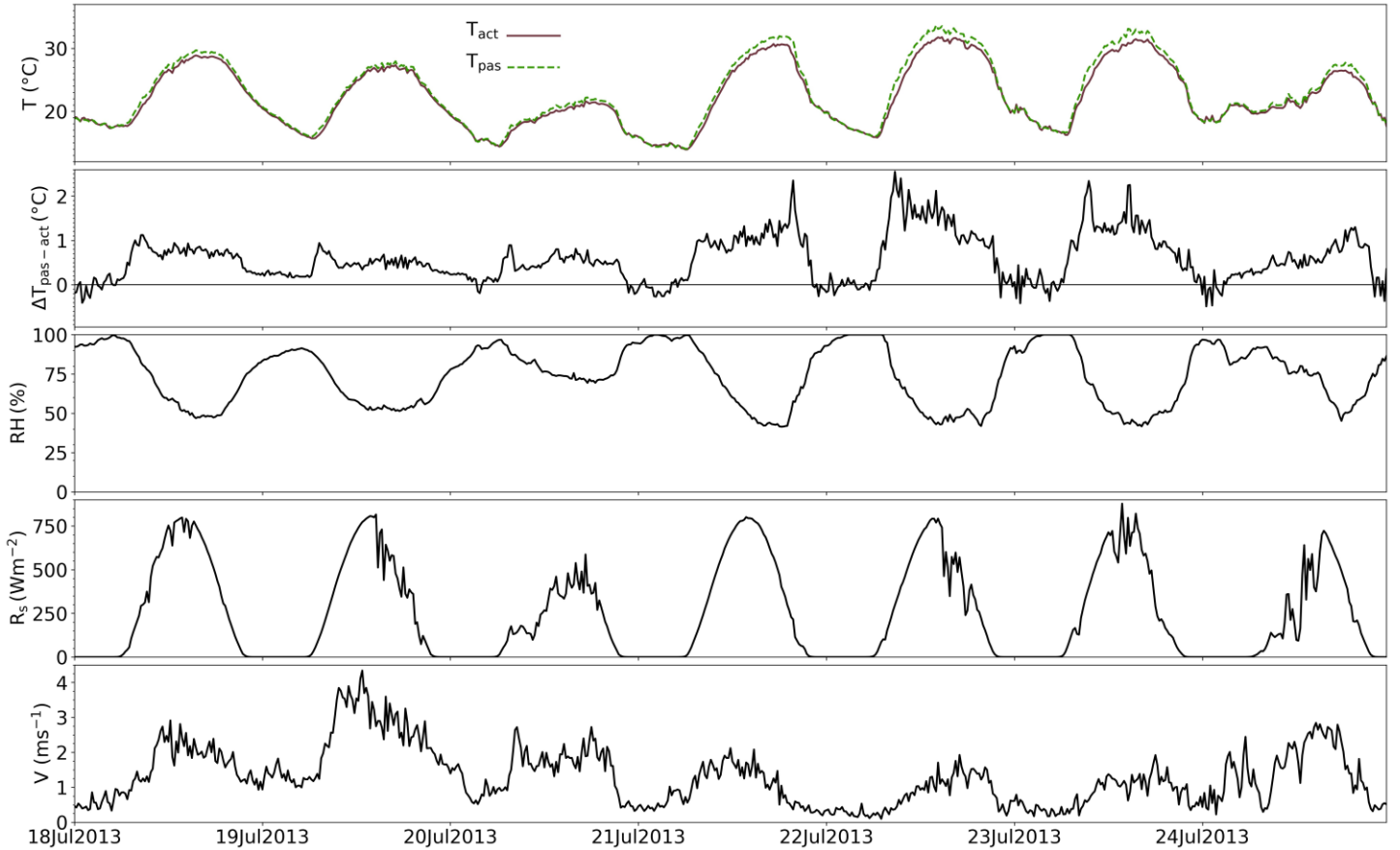


Figure 4. As in Figure 3, but for the rural station.

Table 3 summarises a set of statistics of the differences between the passively minus the actively ventilated measurements for the urban and rural sites. Use is made of the mean bias and root mean square difference, defined respectively as

$$BIAS = \frac{1}{N} \sum_{i=1}^N (T_{pas,i} - T_{act,i}) \quad (1)$$

$$RMSD = \left[\frac{1}{N} \sum_{i=1}^N (T_{pas,i} - T_{act,i})^2 \right]^{1/2}, \quad (2)$$

where the sum runs over all time steps N in the study, i.e., the whole month of July 2013 at 15-minute time steps. Table 3 shows that the bias between the passively and actively ventilated measurements is slightly below 0.5°C for the daily mean temperature, and near zero (bias below 0.1°C) for the minimum temperature, showing nearly no difference between the urban and rural measurements. The daily maximum temperature shows the largest bias, with a value of 1.31°C at the urban station and 0.86°C at the rural station. The RMSD between passively and actively ventilated measurements is close to 0.7°C for the daily mean temperature and near 0.2°C for the minimum temperature, again exhibiting very small differences between the urban and rural measurements. As before, the daily maximum temperature displays the largest RMSD values, that is, 1.37°C at the urban and 0.94°C at the rural location.

Table 3. Statistical indicators related to the differences between certain temperature-based indicators obtained using the passively minus the actively ventilated measurements. The table contains values of daily mean (T_{avg}), maximum (T_{max}) and minimum (T_{min}) temperature measured in the urban and rural stations, as well as the daily mean and maximum UHI increment. In the lower two rows, differences between the passively and actively measured values are quantified using the mean bias (BIAS) and root mean square difference (RMSD).

	urban			rural			urban – rural	
	T_{avg}	T_{max}	T_{min}	T_{avg}	T_{max}	T_{min}	UHI_{avg}	UHI_{max}
BIAS (°C)	0.47	1.31	-0.06	0.48	0.86	0.07	-0.01	-0.01
RMSD (°C)	0.73	1.37	0.22	0.65	0.94	0.19	0.38	0.35

The bias of the passively minus actively ventilated temperature measurements is strongly affected by solar radiation intensity and wind speed. To assess this, we evaluated the temperature bias with respect to the quantity

$$X_{NM} = \frac{R_s}{\rho_a c_p T_0 V}, \quad (3)$$

which was suggested by Nakamura and Mahrt (2005) as a suitable (non-dimensional) quantity combining the effect of shortwave radiation (R_s) and natural ventilation speed (V), and with $\rho_a = 1.2 \text{ kgm}^{-3}$ the air density, $c_p = 1004 \text{ Jkg}^{-1}\text{K}^{-1}$ the specific heat of air at constant pressure, and $T_0 = 300 \text{ K}$ a reference temperature. Figure 5 shows scatter plots of the passive-minus-active temperature bias versus X_{NM} , with correlation coefficients around 0.75 for both the urban and rural sites. Considering the way X_{NM} is constructed, it shows that high solar radiation intensity combined with low wind speed values tend to enhance the temperature bias, which is of course well known from several of the studies cited in the Introduction.

Figure 5 also shows that the data cloud in the scatter plots exhibits considerable differences between the urban and rural stations, despite their identical set-up, i.e., despite the identical instruments and configuration (relative positions and height). Still, the regression lines are rather similar and would appear to suggest that a shift based on X_{NM} could potentially yield sensible corrections, assuming of course that the quantities driving the correction (solar radiation intensity, wind speed) are available.

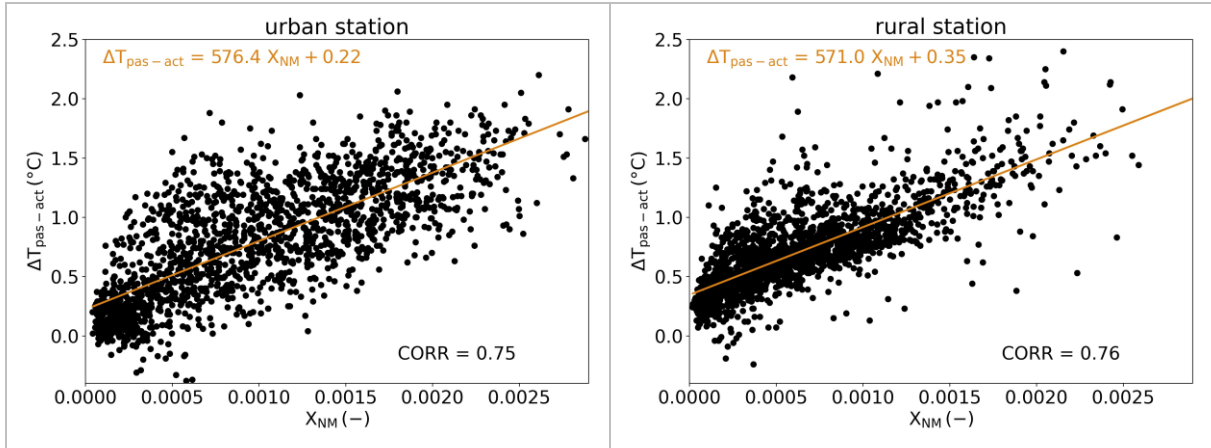


Figure 5. Scatterplots of the temperature bias (passively minus actively ventilated measurements) versus the non-dimensional quantity X_{NM} defined in Eq.(3), for the urban (left) and rural (right) stations. The orange line provides a linear regression through the scatter points, the equation of which is provided on the left top side of each panel.

Note that this positive temperature bias of passively ventilated temperature measurements under a high solar radiation load is also instructive when trying to understand outcomes from measurement campaigns that rely on a large number of sensors distributed over a city, and which typically make use of cheap sensing devices with little or no radiation shielding or active ventilation. The fact that some of the sensors would be (temporarily) shaded may lead to an inaccurate spatial representation of urban air temperature, or to excessive benefits attributed to shading from trees, which in reality attenuate air temperature only to a limited extent. Terando et al. (2017) make a similar observation, and state that, in a large number of ecological studies concerning the attenuating role of urban vegetation, reported temperature reductions are in fact related to shading of the sensors, not lower air temperature.

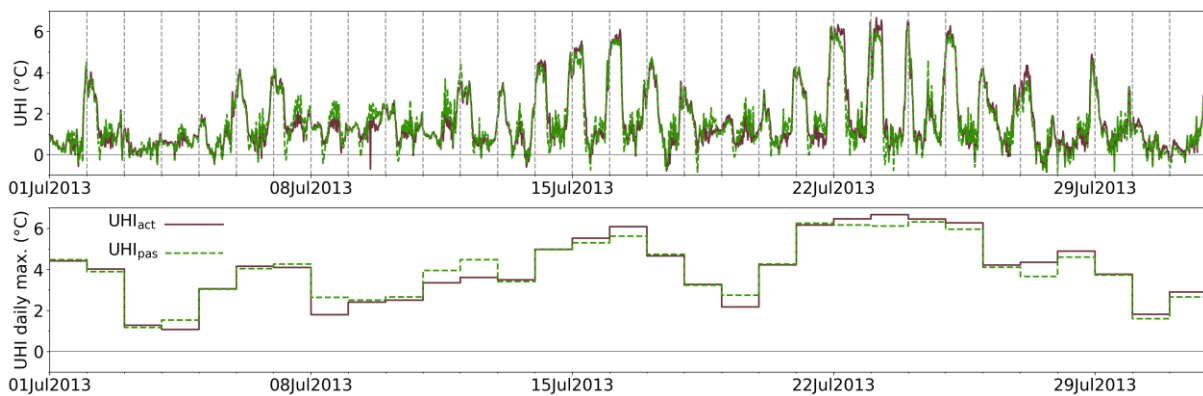


Figure 6. Urban canopy heat island (UHI) intensity during the month of July 2013, derived from the actively (purple) and passively (green) ventilated temperature measurements. The upper panel shows the values at the native 15-minute time resolution; the lower panel displays the daily maximum UHI intensity derived from it. The vertical dashed lines in the upper graph are positioned at midnight, as an aid to identify the timing of the occurrence of the maximum UHI intensity within a day.

Figure 6 shows the UHI increment, calculated as the difference between the urban and rural temperatures measured during the study period. Once more, a clear diurnal cycle is present, the maxima of the UHI intensity occurring during the night in the early hours, and reaching values exceeding 6°C. Strikingly, the UHI increment values obtained from either the passively or the actively ventilated temperature measurements are rather similar. This can be understood by the fact that the passively-minus-actively measured temperature difference is largely a daytime phenomenon, increasing under intense solar radiation and low wind speeds (Figure 3 and Figure 4). Conversely, the highest UHI increments occur at night, when measured temperature is the least affected by the ventilation method.

This limited effect of the ventilation method on the UHI intensity is confirmed in Table 3, the UHI increment showing nearly no bias (less than 0.01°C in magnitude). The RMSD of the UHI increment between the passively and actively ventilated temperature measurements is also small, with values of 0.38°C and 0.35°C for the daily average and maximum UHI increment, respectively. Compared to the magnitude of the UHI increment itself, which at times exceeds 6°C, the temperature bias stemming from the ventilation method is modest.

However, things are different when considering absolute (stand-alone) temperature-based indicators, i.e., indicators not relying on urban-rural temperature differences. To illustrate this, we consider the ‘heatwave degree days’ (*HWDD*) indicator (Brouwers et al., 2015), defined as

$$HWDD = \sum_{i=1}^D \left[(T_{min,i} - 18.2^{\circ}\text{C})^+ + (T_{max,i} - 29.6^{\circ}\text{C})^+ \right] h_i, \quad (4)$$

where the index i in the sum runs over all days (D) in the considered period (here the month of July 2013), and $T_{min,i}$ and $T_{max,i}$ are the daily minimum and maximum temperatures occurring on day i . The ‘+’ superscript means that only positive values are retained, and h_i takes a value of 1 on heatwave days and 0 otherwise. For the present study, a heatwave is defined following the specification of the Belgian Scientific Institute of Public Health, as a period of at least three consecutive days during which, on average, the thresholds of 18.2°C (for T_{min}) and 29.6°C (for T_{max}) are both exceeded (Brits et al., 2010). By its definition, this indicator provides an aggregate picture of the total duration and weight of heat waves throughout a selected period. Following an extensive analysis, Mudelsee (2020) concluded that this type of indicator satisfies a number of criteria with respect to aggregating capability and relevance in the context of human exposure to excessive heat. Among other things, the *HWDD* is routinely used for assessing urban-rural heat increments for the Flemish Environment Agency (Brouwers et al., 2015).

Figure 7 shows the daily minimum and maximum temperatures for the study period, for the urban and rural stations, based on both the actively and passively ventilated temperature measurements. The grey zones in the graphs of the urban station correspond to heatwave periods, according to the definition provided above. Clearly, the passively ventilated measurements identify more heatwave days than the actively ventilated ones, which can be mainly ascribed to the measured higher daytime maximum temperatures, exceeding the 29.6°C threshold more easily. Conversely, night-time temperatures differ little between the actively and passively ventilated measurements. In the rural station, no heatwave is detected, neither in the actively nor in the passively ventilated temperature data.

On top of each panel in Figure 7, *HWDD* values are provided, yielding 19.5°C.d and 31.3°C.d for the actively resp. passively ventilated measurements in the urban station. Note that these *HWDD* values arise entirely during the heatwave days, which are marked in Figure 7 with a shaded background. The larger *HWDD* values, i.e., the values emerging from the passively ventilated measurements, therefore

not only stem from higher daytime maximum temperatures, but also from the induced longer heatwave periods, contributing more terms in Eq. (4).

It is worth noticing that the UHI increment appears to be stronger during heatwave episodes. This is particularly clear during the heatwave found in the urban measurements in the period 21-26 July 2013 (Figure 7), the UHI increment rising to 6°C and more (Figure 6). Such a behaviour, which was also found in other studies (Li and Bou-Zeid, 2013; De Ridder et al., 2017), emphasises the role of the urban heat island in adding to already high heat stress values occurring during heatwave episodes. This also becomes apparent when comparing the heat stress (*HWDD* indicator) found in the urban versus that of the rural station (Figure 7), or from the fact that – during the study period – the urban station registered a heatwave while the rural station did not (see the shading in Figure 7).

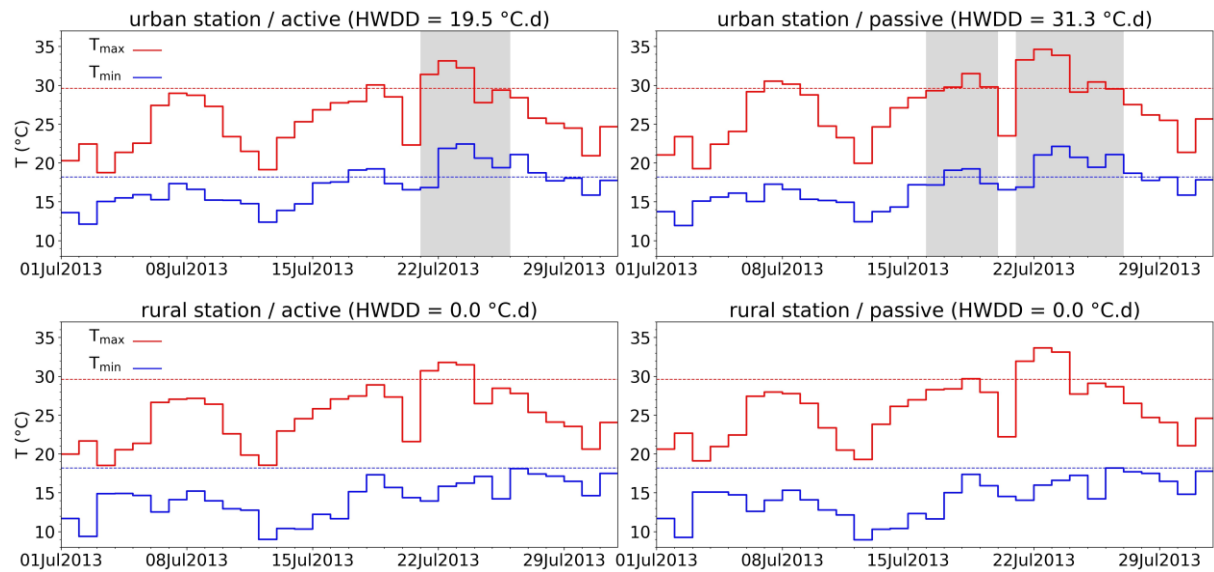


Figure 7. Daily maximum (red) and minimum (blue) temperature at the urban (upper panels) and rural (lower panels) stations for the month of July 2013, based on actively (left) and passively (right) ventilated temperature measurements. The shaded areas correspond to periods identified as heatwaves according to the definition following Eq. (4). Heatwave degree day (*HWDD*) values are shown on top of each panel (units of °C.d).

We also evaluated the effect of passive versus active ventilation for another heat indicator: Steadman’s (1984) apparent temperature (*AT*, units of °C). We used the ‘full’ version of this indicator, which accounts not only for ambient temperature (*T*, in °C), but also for humidity (vapour pressure *e*, in kPa), wind speed (*V*, in ms^{-1}) and ‘net extra radiation’ (Q_g , in Wm^{-2}), as follows:

$$AT = -1.8^\circ\text{C} + 1.07T + 2.4e - 0.92V + 0.044Q_g. \quad (5)$$

The latter variable is given by $Q_g \approx 0.139 R_s$ (derived from Section 2k in Steadman (1984)), with R_s the global (i.e., direct plus diffuse) solar radiation incident on a horizontal plane. In this expression, vapour pressure *e* was calculated from the measured relative humidity and a calculation of the saturated value using Bolton’s (1980) parameterization: $e_s = 0.6112 \exp(17.67 T / (T + 243.5))$.

Figure 8 shows daily maximum and minimum *AT* values for the period studied. We find that values based on passively ventilated air temperature exceed those of the actively ventilated measurements by up to 2.3°C. To get a sense for what this implies in terms of perceived human heat stress, using Eq. (5) it can be verified that a daytime *AT* excess of the order of 2.3°C equates to

- an additional 380 Wm^{-2} incident solar radiation,
- a decrease in wind (ventilation) speed by 2.5 ms^{-1} , or
- an increase of relative humidity by 25 percent-point (considering a base temperature of 30°C),

each of which would be readily sensed by the human body as causing a non-negligible amount of additional heat stress. While we should not generalize this outcome to other heat stress indicators such as the UTCI or PET, it is likely that the latter would suffer similar biases when based on passively ventilated air temperature measurements.

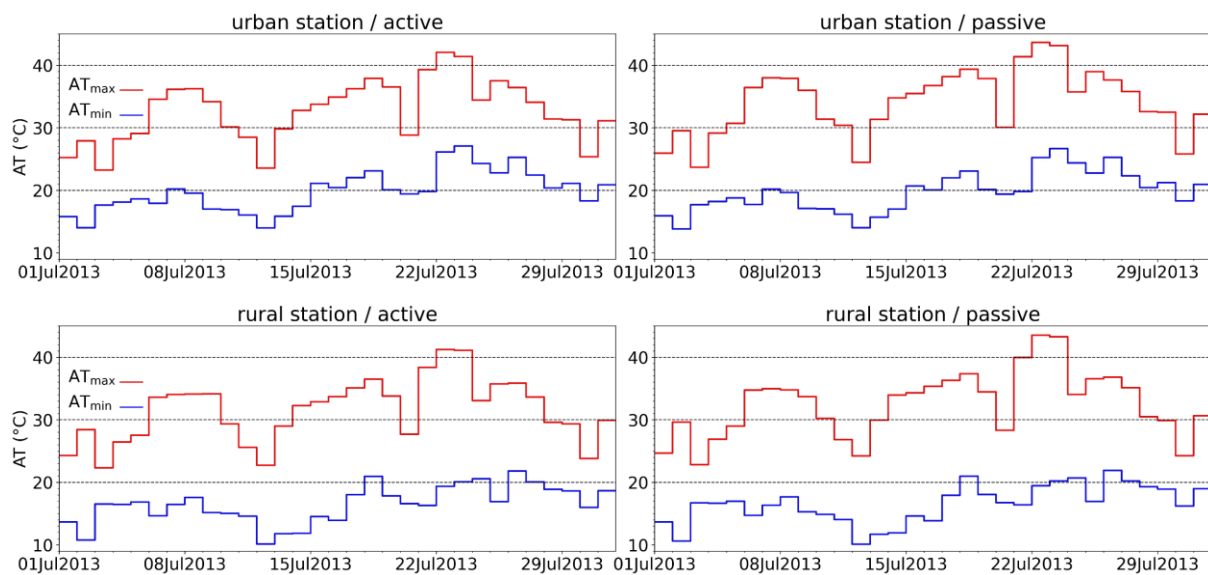


Figure 8. Daily maximum (red) and minimum (blue) apparent temperature (AT) at the urban (upper panels) and rural (lower panels) stations for the month of July 2013, based on actively (left) and passively (right) ventilated temperature measurements.

4 Conclusions

We presented surface air temperature values measured at an urban and a nearby rural site in Antwerp, Belgium, during the month of July 2013. In each of the climate stations, temperature measurements were gathered in both passively and in actively ventilated radiation shields, thus allowing an assessment of the differences resulting from the two methods. In our study, these temperature differences were assessed in terms of their effect on air temperature-based urban heat (island) indicators.

It was found that passively minus actively measured temperature differences reached up to about 2°C, in good agreement with results obtained by other workers. The highest values occurred under high solar radiation loads, meaning that – overall – night-time temperature biases are much lower than daytime biases.

As a result, the urban heat island (UHI) increment, which during the study period reached values of around 6°C, was found to differ little between the passively and actively ventilated methods, largely because the highest UHI values are typically reached at night when the ventilation method does not affect the measured temperature much. Conversely, the heatwave degree days (*HWDD*) indicator, which is relevant in, e.g., climate-health assessments, at times showed a strong sensitivity to the ventilation method, i.e., passive versus active. The main explanation was that this indicator contains daily maximum temperature as an important contributor, which often strongly differs between passively and actively ventilated measurements, especially under the conditions found during heatwaves, i.e., strong insolation and low wind speeds. A similar conclusion was drawn concerning the effect of active versus passive ventilation on Steadman's (1984) apparent temperature, for which the

positive temperature bias of a passively ventilated measurement had a similar effect on perceived heat stress as several hundred Wm^{-2} of additional solar radiation load.

To wrap up, the evidence contained in the measurements presented above leads to the conclusion that, while the ventilation method may not matter much when considering the UHI increment, it does when heat indicators are constructed that involve daytime temperatures. In that case, urban heat indicators are prone to yield unrealistically high values when based on measurements obtained in passively ventilated set-ups.

As a follow-up of the study presented here, we are currently engaged in new experimental work that considers the impact of the ventilation method on temperature differences between tree-shaded sites versus fully exposed (to solar radiation) locations, in order to better understand the true beneficial effect of urban trees in terms of local air temperature attenuation.

Acknowledgements

We are grateful to the Koninklijk Lyceum Antwerpen and Biofarm Van Leemputte in Vremde for kindly hosting the climate stations used in this study. The maps shown in Figure 9 were obtained from Geopunt Vlaanderen (1-m land cover map for 2012, <https://www.geopunt.be/>). Finally, we would like to acknowledge the enriching discussions and follow-on projects we had with the Flemish Environment Agency.

References

- Anderson, S. P., & Baumgartner, M. F., 1998. Radiative heating errors in naturally ventilated air temperature measurements made from buoys. *J. Atmos. Oceanic Technol.*, 15, 157-173. [https://doi.org/10.1175/1520-0426\(1998\)015%3C0157:RHEINV%3E2.0.CO;2](https://doi.org/10.1175/1520-0426(1998)015%3C0157:RHEINV%3E2.0.CO;2)
- Bolton, D., 1980. The computation of equivalent potential temperature. *Monthly Weather Review*, 108, 1046-1053. [https://doi.org/10.1175/1520-0493\(1980\)108<1046:TCOEPT>2.0.CO;2](https://doi.org/10.1175/1520-0493(1980)108<1046:TCOEPT>2.0.CO;2)
- Brits, E., I. Boone, B. Verhagen, M. Dispas, H. Van Oyen, Y. Van Der Stede, A. Van Nieuwenhuysse, 2010. Climate change and health: Set-up of monitoring of potential effects of climate change on human health and on the health of animals in Belgium. Scientific Institute of Public Health, Unit Environment and Health, Brussels, Belgium, 54 pp.
- Brouwers J., Peeters B., Van Steertegem M., van Lipzig N., Wouters H., Beullens J., Demuzere M., Willems P., De Ridder K., Maiheu B., De Troch R., Termonia P., Vansteenkiste Th., Craninx M., Maetens W., Defloor W., Cauwenberghs K., 2015. MIRA Climate Report 2015, about observed and future climate changes in Flanders and Belgium. Flanders Environment Agency in collaboration with KU Leuven, VITO and RMI. Aalst, Belgium, 147 pp.
- Cheng, X., Su, D., Li, D., Xu, W., Yang, M., Li, Y., Yue, Z., Wang Z., 2014. An improved method for correction of air temperature measured using different radiation shields. *Adv. Atmos. Sci.*, 31, 1460–1468. <https://doi.org/10.1007/s00376-014-3129-0>
- De Ridder, K., D. Lauwaet, B. Maiheu, 2015. UrbClim – a fast urban boundary layer climate model. *Urban Climate*, 12, 21-48. <https://doi.org/10.1016/j.uclim.2015.01.001>
- De Ridder K, Maiheu B, Lauwaet D, Daglis IA, Keramitsoglou I, Kourtidis K, Manunta P, Paganini M., 2017. Urban heat island intensification during hot spells—the case of Paris during the summer of 2003. *Urban Science*, 1:3. <https://doi.org/10.3390/urbansci1010003>
- Erell, E., Leal, V. & Maldonado, E., 2005. Measurement of air temperature in the presence of a large radiant flux: an assessment of passively ventilated thermometer screens. *Boundary-Layer Meteorol.*, 114, 205–231. <https://doi.org/10.1007/s10546-004-8946-8>
- Georges, C., and Kaser, G., 2002. Ventilated and unventilated air temperature measurements for glacier-climate studies on a tropical high mountain site, *J. Geophys. Res.*, 107, 4775, <https://doi.org/10.1029/2002JD002503>
- Gubler, M., A. Christen, J. Remund, S. Brönnimann, 2021. Evaluation and application of a low-cost measurement network to study intra-urban temperature differences during summer 2018 in Bern, Switzerland. *Urban Climate*, 37, 100817. <https://doi.org/10.1016/j.uclim.2021.100817>
- Huwald, H., Higgins, C. W., Boldi, M.-O., Bou-Zeid, E., Lehning, M., and Parlange, M. B., 2009. Albedo effect on radiative errors in air temperature measurements, *Water Resour. Res.*, 45, W08431, <https://doi.org/10.1029/2008WR007600>
- Lauwaet, D., B. Maiheu, J. Aertsens, K. De Ridder, 2013. Opmaak van een hittekaart en analyse van het stedelijk hitte-eiland effect voor Antwerpen (in Dutch). Study conducted under the authority of the City of Antwerp, VITO report 2013/RMA/R/352, 234 pp. (available from <https://www.antwerpenmorgen.be/files/download/66130141-d647-4b7f-848a-81c211241a61>).

- Li, D. and Bou-Zeid, E., 2013. Synergistic interactions between urban heat islands and heat waves: the impact in cities is larger than the sum of its parts. *J. Appl. Meteorol. Climatol.*, 52, 2051–2064. <https://doi.org/10.1175/JAMC-D-13-02.1>
- Mauder, M., R. L. Desjardins, and R. Haarlem, 2008. Errors of naturally ventilated air temperature measurements in a spatial observation network. *J. Atmos. Oceanic Technol.*, 25, 2145–2151, <https://doi.org/10.1175/2008JTECHA1046.1>
- Morino, S., Kurita, N., Hirasawa, N., Motoyama, H., Sugiura, K., Lazzara, M., Mikolajczyk, D., Welhouse, L., Keller, L., & Weidner, G., 2021. Comparison of ventilated and unventilated air temperature measurements in inland Dronning Maud Land on the East Antarctic Plateau. *Journal of Atmospheric and Oceanic Technology*, 38, 2061-2070. <https://doi.org/10.1175/JTECH-D-21-0107.1>
- Mudelsee, M., 2020. *Statistical analysis of climate extremes*. Cambridge University Press, Cambridge, UK, 200 pp. <https://doi.org/10.1017/9781139519441>
- Nakamura, R. and Mahrt, L., 2005. Air temperature measurement errors in naturally ventilated radiation shields. *Journal of Atmospheric and Oceanic Technology*, 22, 1046-1058. <https://doi.org/10.1175/JTECH1762.1>
- Ramesh, N.T., Arakeri, J.H., 2019. Actively and passively aspirated temperature sensors in a windless environment like greenhouses. *Sādhanā* 44, 91. <https://doi.org/10.1007/s12046-019-1066-4>
- Steadman, R.G., 1984. A universal scale of apparent temperature. *J. Appl. Meteorol. Climatol.*, 23, 1674–1687. [https://doi.org/10.1175/1520-0450\(1984\)023<1674:AUSOAT>2.0.CO;2](https://doi.org/10.1175/1520-0450(1984)023<1674:AUSOAT>2.0.CO;2)
- Stewart, I. D. and Oke, T. R., 2012. Local climate zones for urban temperature studies. *Bulletin of the American Meteorological Society*, 93, 1879-1900. <https://doi.org/10.1175/BAMS-D-11-00019.1>
- Terando, AJ, Youngsteadt, E, Meineke, EK, Prado, SG, 2017. Ad hoc instrumentation methods in ecological studies produce highly biased temperature measurements. *Ecol Evol.* 7, 9890–9904. <https://doi.org/10.1002/ece3.3499>
- Verdonck, M. L., Okujeni, A., van der Linden, S., Demuzere, M., De Wulf, R., & Van Coillie, F., 2017. Influence of neighbourhood information on “Local Climate Zone” mapping in heterogeneous cities. *International Journal of Applied Earth Observation and Geoinformation*, 62, 102–113. <http://dx.doi.org/10.1016/j.jag.2017.05.017>
- WMO, 2018. *Guide to instruments and methods of observation*. Volume I: Measurement of meteorological variables. World Meteorological Organization, WMO-No.8, 548 pp.

Appendix. Additional specifications concerning the experimental sites

This Appendix provides extra information regarding the urban and rural experimental site characteristics. Figure A1 shows a map with the spatial distribution of LCZ categories in the study area. Figure A2 provides pictures of both stations, including a view of their surroundings.

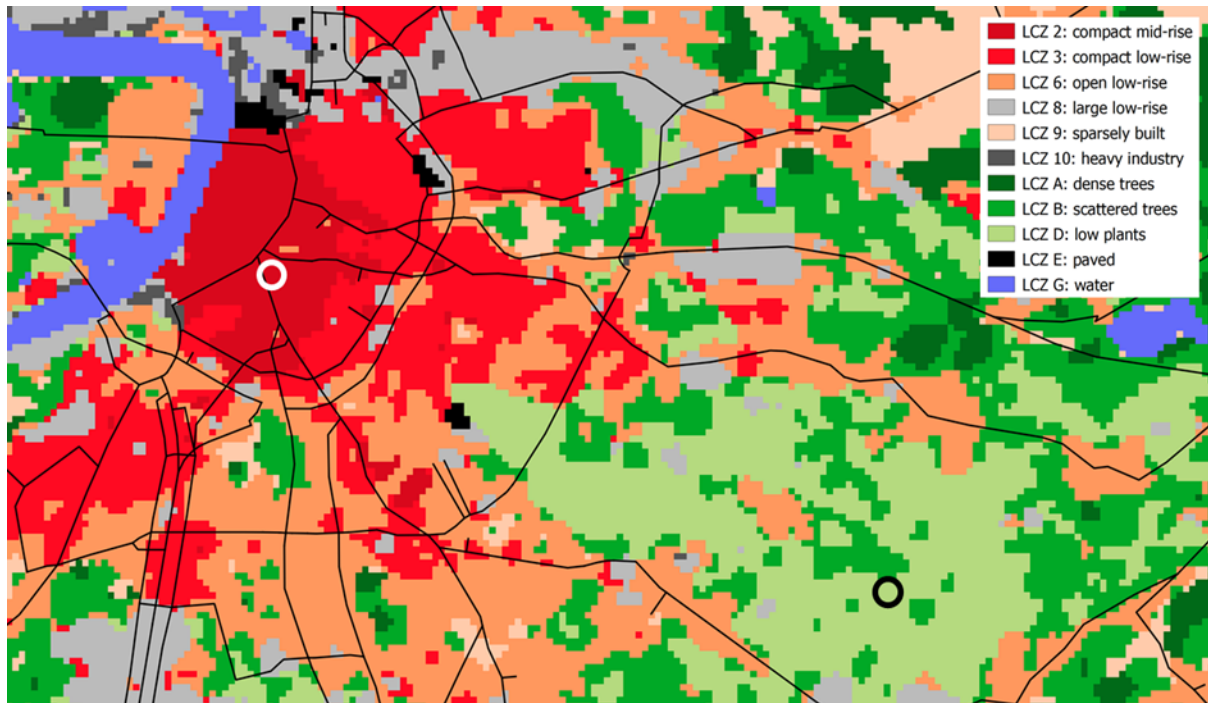


Figure A1. Land cover categories according to the Local Climate Zones (LCZ) classification. The urban station (white circle) is within an area labelled as 'LCZ2: compact mid-rise', and the rural station (black circle) is situated amidst 'LCZ D: low plants'. Source: LCZ data from Verdonck et al. (2017).



Figure A2. Photographs displaying the urban (left) and rural (right) climate stations and their surroundings.